

Fine Structure in the $C^{12}(\gamma,n)C^{11}$ and $O^{16}(\gamma,n)O^{15}$ Activation Curves

L. KATZ, R. N. H. HASLAM, R. J. HORSLEY, A. G. W. CAMERON, AND R. MONTALBETTI
Department of Physics, University of Saskatchewan, Saskatoon, Canada

(Received April 7, 1954)

A careful examination of the $C^{12}(\gamma,n)C^{11}$ and $O^{16}(\gamma,n)O^{15}$ reactions, resulting from irradiating samples with betatron bremsstrahlung, has revealed discontinuities in the yields as a function of peak bremsstrahlung energy. These discontinuities are interpreted to indicate the presence of strong photon absorption levels in the C^{12} and O^{16} nuclei. In C^{12} the discontinuities were found at 19.3, 19.8, 20.1, 20.5, 20.7, 21.1, 21.6, 22.4, and 22.8 Mev, and in O^{16} they were found at 15.9, 16.4, 16.7, 16.9, 17.1, 18.9, 19.3, 20.7, and 21.9 Mev. The experimental results are discussed in detail and are interpreted qualitatively.

INTRODUCTION

THE work grew out of a calibration of the energy scale of the University of Saskatchewan 25-Mev betatron, following a modification in the integrator-expander circuit of this machine¹ early in 1952. It happened that more points were taken at smaller energy intervals near the threshold of the $O^{16}(\gamma,n)O^{15}$ reaction than had been the previous practice. Several well-defined discontinuities in slope were found in a plot of the induced O^{15} , 2.0-minute positron activity against betatron operating energy.

Further work has shown that the energies at which these discontinuities ("breaks") occur are reproducible to within experimental accuracy. Early measurements showed that the first four breaks of the $O^{16}(\gamma,n)O^{15}$ activation curve were reproducible under varying experimental conditions. Five separate experiments involving such changes as reference voltage in the integrator expander and helipot potentiometer gave reproducible results.² Since then further breaks have been found at higher energies in the $O^{16}(\gamma,n)O^{15}$ reaction. Breaks have also been found in the $C^{12}(\gamma,n)C^{11}$ activation curve and in similar curves for other light elements in the region up to calcium. They have not been resolved in elements as heavy as copper. In the light elements they have been found in experiments in which the residual activity was measured as well as in experiments in which the neutrons resulting from the reaction were detected. It has been shown that the "break" energies are not functions of the instrumentation of the betatron. In this paper the work on the $C^{12}(\gamma,n)C^{11}$ and $O^{16}(\gamma,n)O^{15}$ reactions will be reported since these two reactions are the most extensively investigated to date. Other reactions are reported in the accompanying paper.

The breaks in our activation curves are apparently of the same nature as those found by Miller and Waldman³ in the excitation of low-energy levels in indium by x-rays. The straight line portions observed by those workers in their activation curves were inter-

preted by Guth⁴ in terms of thick-target spectra. The implications of similar straight line portions in our results are not yet clearly understood. We believe the breaks indicate that in the light nuclei photon absorption takes place, at least in part, into well-defined nuclear levels of the target nucleus. It is suspected that the "line" absorption indicated by the breaks is superimposed on a continuum of absorption which constitutes the experimentally well-established "giant-resonance."

EXPERIMENTAL TECHNIQUE

The basic experiment consists of the irradiation of a number of samples at various betatron energies. However, to establish the fine structure it is necessary that the activities induced in the various samples be determined very accurately relative to one another and that the energies of the irradiation be held steady to within a few kiloelectron volts.

For the oxygen activation curve cylindrical samples of boric acid ($H_2B_4O_7$) were used. These were formed by compressing the boric acid powder without binder, under a pressure of about 7 ton/in.² The cylinders were about 5 cm long, 2.2-cm inside and 4.0-cm outside diameter. The carbon samples were cut from polystyrene tubes 2.6-cm outside diameter and 2-mm wall thickness. They were 7.5 cm long.

The samples were counted with Victoreen IB85 cylindrical Geiger counters, over which they had been designed to fit with a slight clearance. Usually two setups were used with the oxygen samples and up to four with the carbon samples. These were intercalibrated by moving a sample among them as its activity decayed.

The samples were irradiated in the betatron beam with the cylindrical axis parallel to the beam. Each sample was given a definite irradiation dose as measured by an ionization chamber whose output was integrated. The time of irradiation for each sample was carefully measured.

The activity induced in the oxygen samples (O^{15}) has a half-life of 2.0 minutes. The counting started one minute after the end of irradiation and continued for four minutes. In the case of carbon samples the

¹ Katz, McNamara, Forsyth, Haslam, and Johns, Can. J. Research A28, 93 (1950).

² Haslam, Katz, Horsley, Cameron, and Montalbetti, Phys. Rev. 87, 196 (1952).

³ W. C. Miller and B. Waldman, Phys. Rev. 75, 425 (1949).

⁴ E. Guth, Phys. Rev. 59, 325 (1941).

induced activity (C^{11}) has a half-life of 20.5 minutes. The counting of these started 10 minutes after the end of irradiation and continued for 10 minutes. The total number of counts which were recorded in each of these periods (less tube background) when corrected for irradiation time was taken as representing the activity induced in the samples.

Care was taken during each irradiation to hold the dose rate from the betatron constant. However, the dose rate varies by a factor of ten as the betatron operating energy is changed by a factor of two. Thus, the irradiation time t_R required to give a definite dose of irradiation Q to the samples at different energies varied. The average photon flux incident on a sample in a given irradiation is Q/t_R . Thus, the recorded number of counts were corrected to unit dose rate (arbitrary) and to saturation by multiplying each reading by $t_R/[1-\exp(-\lambda t_R)]$.

BETATRON ENERGY STABILITY

Experience has shown that an instability in the operating energy of the betatron of 40 to 50 keV will cause the experimental points to scatter so badly that all but the strongest breaks in the activation curve will be smeared out. It has been found that under favorable operating conditions the stability of the betatron energy is better than ± 5 keV. In our early work on

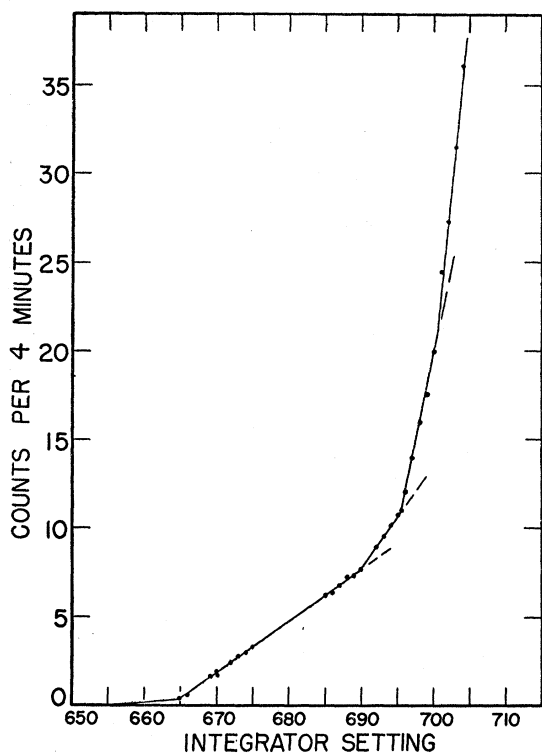


FIG. 1. $O^{16}(\gamma, n)O^{15}$. Oxygen activation curve near threshold. The fast-rising portion of this curve has a slope corresponding to an increase of 5 percent in counting rate per 10-keV change in peak bremsstrahlung energy.

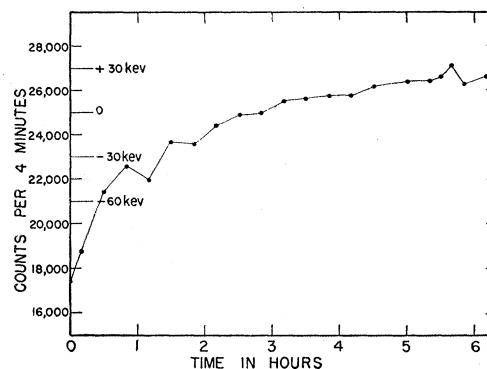


FIG. 2. Betatron energy stability. After the initial warmup period, the peak bremsstrahlung energy remained constant to ± 5 keV, except for the slow drift, over a period of a few hours.

the fine structure in activation curves, these good operating conditions were erratically obtained, and it was often necessary to check the stability by the method outlined below. Recently, however, the factors limiting the betatron stability have in the main been delineated and improved, and it is now possible to obtain satisfactory measurements at any time.

A part of the oxygen activation curve near threshold is reproduced in Fig. 1. In this region the induced activity is a strong function of the betatron operating energy. It is possible to choose a point on this curve for monitoring the betatron energy which is sufficiently far from threshold to give good counting statistics and yet show an increase of five percent in activity for a change of 10 keV in energy. The results of one of our early experiments to measure betatron stability are shown in Fig. 2. The boric acid samples were irradiated at constant energy setting and were given the same irradiation dose. The initial rising portion of the curve is interpreted as a drift in operating energy resulting from warming up of the betatron magnet or a drift of the reference voltage of the integrator-expander circuit. After this initial period the energy remained constant to within ± 5 keV (2 percent change in counting rate or about 500 counts). The slow residual energy drift is easy to detect⁵ and to correct for.

EXPERIMENTAL RESULTS

The earliest sets of measurements of the oxygen and carbon activities usually extend over relatively small energy intervals owing to the tendency of the betatron to lose its good energy stability after a few hours of running time. Also, on different days there was a tendency for the "zero point" of the energy scale to shift slightly with respect to the setting of the integrator helipot. For these reasons, the usual technique in a given set of measurements was to remeasure the energy position of a previously known break and then to measure as much more of the activation curve as

⁵ Robinson, McPherson, Greenberg, Katz, and Haslam (to be published).

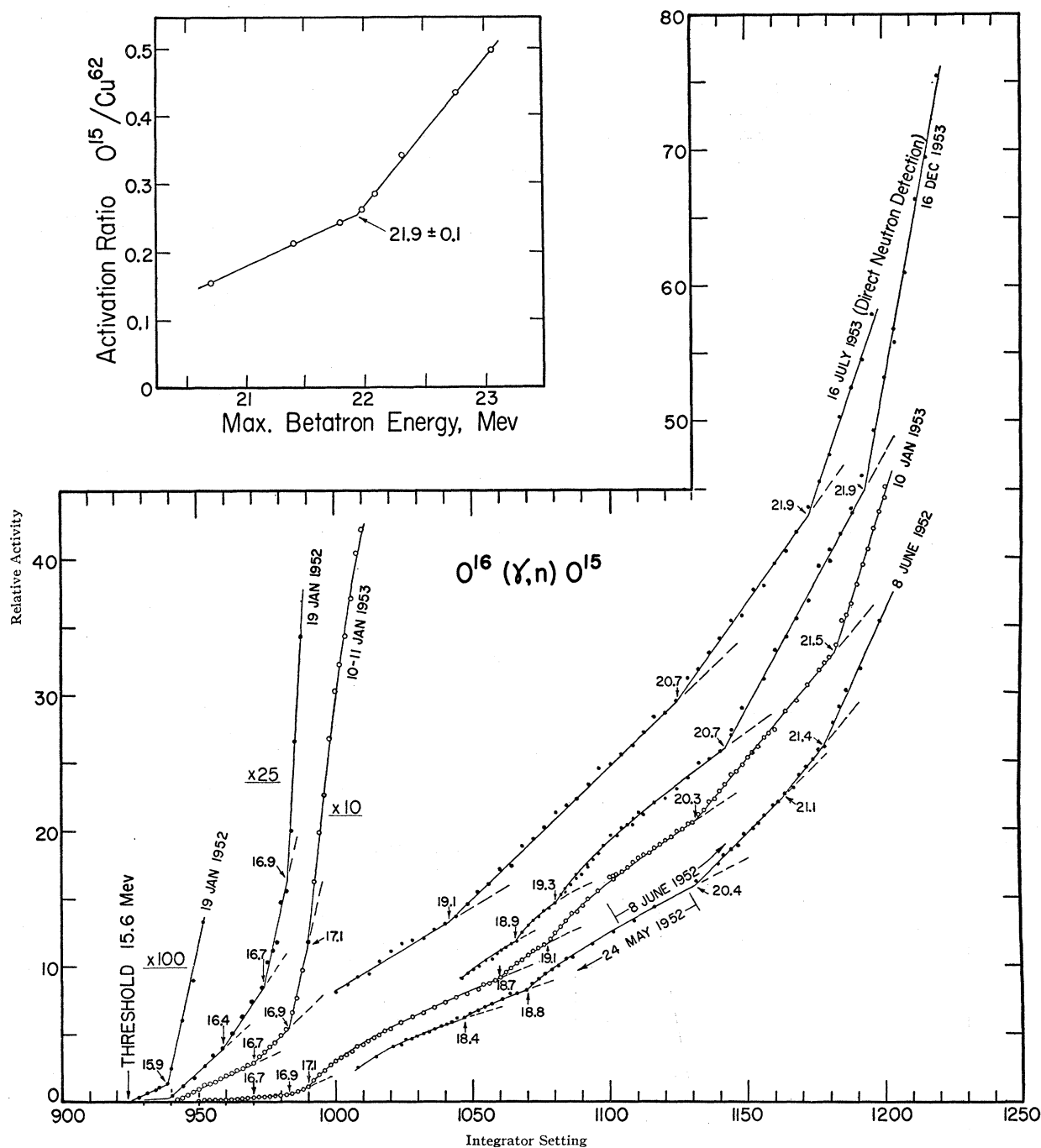


Fig. 3. Oxygen activation curves taken at intervals of approximately 6 months over a period of two years. The energy scale of the betatron was established most reliably in the latter part of 1953 and the positions of the breaks in the high-energy region are to be taken from the curves of July and December, 1953. The break at 21.9 Mev shown in the insert was obtained by irradiating copper and oxygen samples simultaneously and plotting the ratio of the induced activities.

possible before the betatron became unstable. Thus, in order to build up a composite activation curve from the early measurements, it has been necessary to normalize these separate runs both in energy and intensity.

In Fig. 3, we show representative curves of the

$O^{16}(\gamma, n)O^{15}$ reaction taken at intervals of approximately 6 months over a period of two years. The initial portion of the curve was established with great care in our early measurements, and only the curves taken on January 19, 1952, and January 10, 1953, are shown. All the curves except the one of July 16, 1953, were

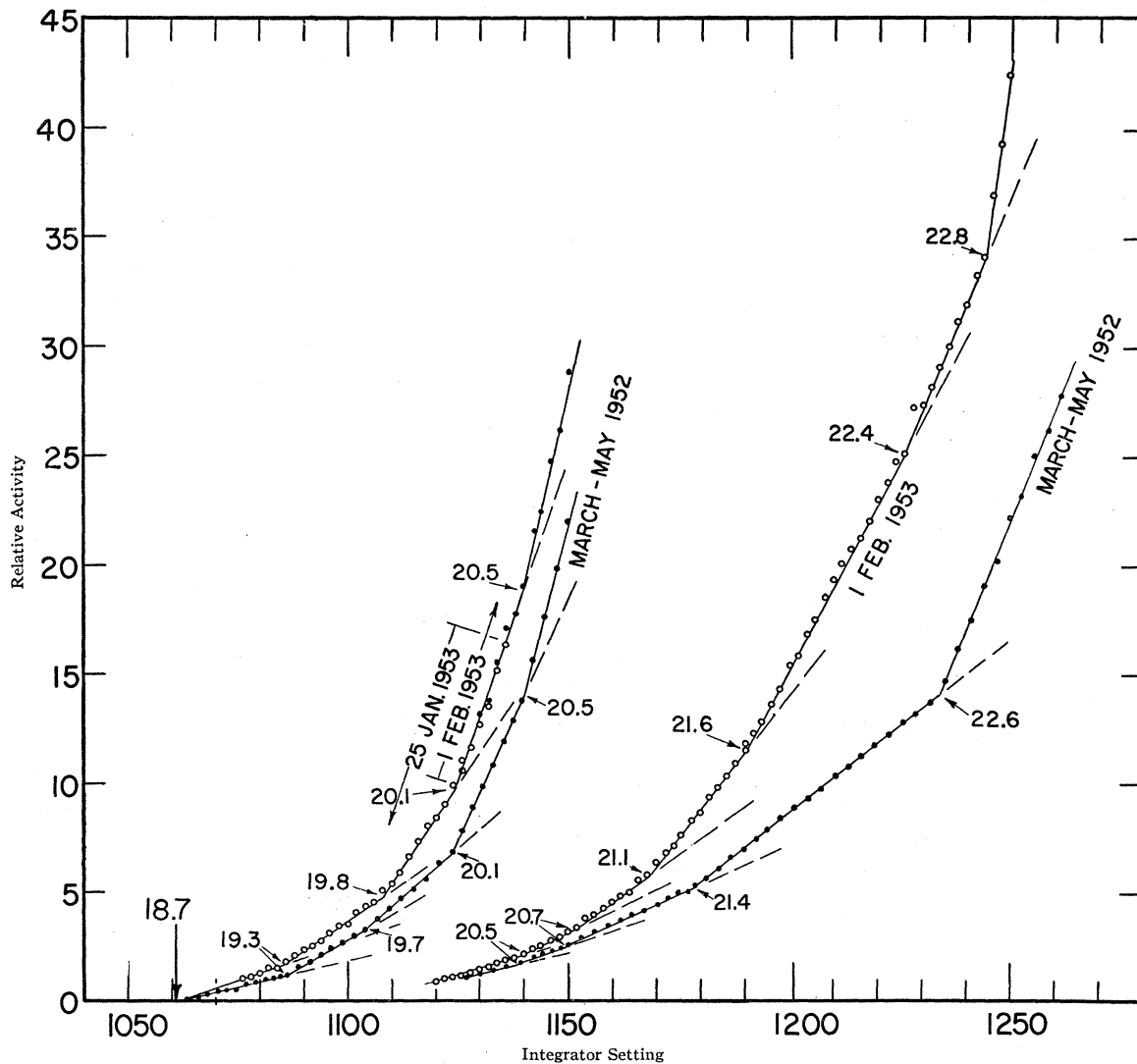


FIG. 4. $C^{12}(\gamma, n)C^{11}$ residual activity. Carbon activation curves. The early set of measurements extended over a two-month period, and only the composite curve is shown. The low-energy region of the newer curve was taken in one continuous run on January 25, 1953, and the high-energy portion on February 1. In two cases a single level in the older curve was resolved into two weaker levels by the February 1 measurements.

obtained by measuring the induced O^{15} β -ray activity. The curve of July 16 was obtained by detecting the neutrons emitted in the (γ, n) reaction. Because of poorer sensitivity the low-energy region of this curve could not be obtained and the two breaks at 18.9 and 19.3 Mev could not be resolved separately but gave one break at an intermediate energy.

Since the $O^{16}(\gamma, n)O^{15}$ threshold has always been one of the calibration points on our energy scale, the positions of the breaks in the low-energy portion of Fig. 3 are probably known to within ± 0.1 Mev. On the other hand, the positions of the breaks in the high-energy region are based on an extrapolation of our energy scale and are thus not known nearly as accurately—certainly not better than ± 0.2 Mev. The data of December 16, 1953, are the most reliable; the older

curves are included only to emphasize the reproducibility of the general features of these curves.

The most serious discrepancy in our measurements occurred in a level which the early work placed at 21.5 Mev but which more recent curves show at 21.9 Mev. This particular level has been studied in great detail using our most recent techniques for establishing an accurate betatron energy scale.⁵ In one of the experiments copper and oxygen (boric acid) samples were irradiated simultaneously, then counted alternately with the same G.M. counter. The ratio of the induced O^{15} to Cu^{62} activities resulting from the (γ, n) reactions is shown in the insert of Fig. 3. Each point on the curve represents a total of about 20 000 counts for the oxygen sample and 50 000 counts for the copper sample. The break thus established was found to be at 21.9 ± 0.1

Mev. This break is easy to detect and may be used as a secondary calibration point for the betatron energy scale.

Near threshold the breaks in slope of Fig. 3 are quite sharp and the changes in slope at each break are usually large. Between the breaks the points can be fitted well with straight lines. Under these conditions the detection of the breaks is relatively straightforward and easy. For this reaction the character gradually changes above 17 Mev. The breaks become separated by larger energy intervals, and the activation curve can no longer be well represented by straight lines: it is concave towards the energy axis. At still higher energies (around 21 Mev) the intervening portions of the activation curve are straight once again. An attempt at interpreting these features will be given below.

A composite activation curve for the $C^{12}(\gamma, n)C^{11}$ reaction taken over a three-month period extending from March to May, 1952, is shown in Fig. 4. On the same figure is shown a more recent curve taken on January 25 and February 1, 1953. It is immediately seen that the new data have two cases in which a single previous break has been resolved into two breaks; thus the break at 21.4 Mev now appears as breaks at 21.1 and 21.6 Mev, and the break at 22.6 Mev has been resolved into two breaks at 22.4 and 22.8 Mev. The break at 20.7 Mev has been examined with great care and is shown in Fig. 6 of the accompanying paper. Each point in that figure was established with a counting accuracy of ± 1 percent, and the results clearly indicate the existence of this level. The points in Fig. 4 of this paper were established with equal accuracy though the measurements were spaced somewhat further apart. Actually, the scale used in showing the break at 20.7 Mev in this figure does not do justice to the accuracy of our measurements. The spacing of the breaks for this reaction is more regular than in the case of oxygen, and there is no pronounced concavity towards the energy axis.

DISCUSSION OF RESULTS

It is difficult to estimate the resolving power of this method for detecting a true discontinuity of slope. There will be some scattering of the points on the activation curve owing to energy instability of the betatron and to the finite number of counts which are taken. We estimate that other causes of scattering, such as variations in dose delivered to the sample, differences in samples, or irradiation geometries are negligible compared to the two causes mentioned above. The effect of most of such scattering is to change the appearance of the activation curve from a series of straight segments to a continuous curve. Our experience has shown that an energy instability of ± 50 kev in the energy is sufficient to destroy the evidence for most of the breaks reported here. However, the scattering resulting from an energy instability of ± 5 kev is

usually comparable to that resulting from counting statistics of ± 1 percent. Thus the stability is adequate for the work which can be done with the bremsstrahlung intensities available from our betatron.

Furthermore, in order that a change of slope may readily be detected the change must be comparable to the slope itself below the break. In general, we have found that an increase of slope of much less than 50 percent is almost undetectable with our present techniques. This observational requirement indicates that weak levels can be detected only near threshold and reflects the integral nature of our activation curve. Thus, if we assume that the level giving rise to a break at energy E_i has a photon absorption cross section $\sigma_i(E)$ with a peak value of σ_i^0 , and $\sigma_{\gamma n}(E)$ is the cross section leading to (γ, n) reactions from photon absorption into the giant dipole resonance as well as in all levels except the one at E_i , then the number of activations induced when one mole of sample is irradiated with 100 roentgens is given⁶ by

$$\alpha(E_0) = 0.602 \int_0^{E_0} [\sigma_{\gamma, n} + G\sigma_i] P(E, E_0) dE, \quad (1)$$

where G is the fraction of the photons absorbed into level i which give rise to (γ, n) reactions and $P(E, E_0)$ is the number of photons of energy E per cm^2 per 100 r in the betatron spectrum of maximum energy E_0 .

If we assume that the level is very narrow we can write

$$\alpha(E_0) = 0.602 \int_0^{E_0} \sigma_{\gamma n} P dE + 0.602 G P(E_i, E_0) \int_0^{E_0} \sigma_i dE. \quad (2)$$

The second term on the right-hand side gives the contribution from the level, and thus the change in slope at E_i is proportional to

$$G P(E_i, E_0) \int_0^{E_0} \sigma_i dE / \int_0^{E_0} \sigma_{\gamma n} P dE. \quad (3)$$

The fact that breaks are seen up to over 7 Mev above threshold shows that there are levels at these higher energies which involve an integrated cross section comparable to the total integrated cross section up to that energy.

An additional limitation on the resolving power of the method comes from the spacing of the breaks themselves. It requires at least three points to indicate the linearity of a portion of the activation curve. For a convincing demonstration there should be many more points than this on the linear portion. The natural scattering of the points about such a line makes it difficult to establish either the linearity or the

⁶ L. Katz and A. G. W. Cameron, Can. J. Phys. **29**, 518 (1951).

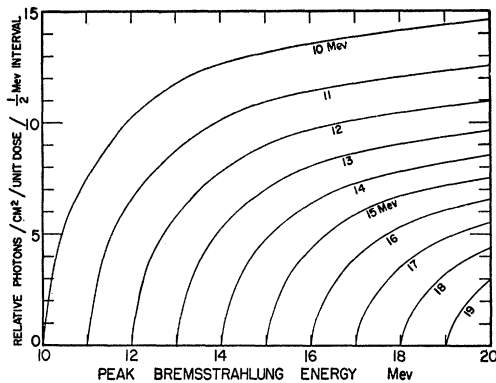


FIG. 5. Isochromats obtained from the theoretical Schiff spectrum shape normalized to unit integrated current from the ion chamber used.

slope of a small energy interval (less than ~ 50 kve; but depending on conditions). One particularly misleading situation can occur when two breaks of comparable strength lie close together. If one is not careful, these will be measured as a single break at an intermediate energy. See, for example, data of July 16, 1953, Fig. 3, which because of poor sensitivity gave a single break at 19.1 Mev instead of levels at 18.9 and 19.3 Mev. There are also two such examples in Fig. 4.

INTERPRETATION OF THE ACTIVATION CURVES

The dependence of the observed activity on photon absorption cross section and bremsstrahlung spectrum is given by Eq. (1). The spectrum $P(E, E_0)$ is usually normalized per "roentgen." However in this experiment the activity has been normalized to an arbitrary unit of integrated current from a transmission ion chamber in the x-ray beam. The data have been left normalized in this way because the doses delivered to the samples were very reproducible when the betatron was controlled by the integrated reading of the ion chamber.

For the purpose of analyzing the principle features of the photonuclear activation curves obtained here, it would be useful to have plots of the isochromats for the spectrum $P(E_i, E_0)$. That is $P(E_i, E_0)$ is plotted as a function of E_0 for given values of E_i , with the photon numbers properly normalized to unit integrated current of the ion chamber. Since our analysis is intended to reveal the fine structure in the photon absorption cross section, the shape of the isochromats near the upper end of the bremsstrahlung spectrum are of particular interest. This is immediately evident from Eq. (3).

To date there are no reliable data on the shape of the bremsstrahlung spectrum near its upper end for a betatron operated with the thick target as supplied by the Allis Chalmers Company and under the conditions of orbit expansion usually used. This spectrum will differ from that predicted theoretically because of energy loss within the thick target by the radiating

electron, secondary bremsstrahlung from electrons which have previously radiated, and multiple traversals of the target by electrons which are captured back into the stable orbit after an initial traversal. A plot of the theoretical spectrum given by Schiff⁷ shows it to be concave to the energy axis near its upper end⁶ with perhaps a slight discontinuity at the peak. The above-mentioned effects would tend to straighten out this concavity resulting in a spectrum which decreases more linearly near its upper end with increasing energy.⁸

With these observations in mind we have plotted the isochromats in Fig. 5 making use of the theoretical Schiff spectrum. The curves were obtained by making a cross plot of the Schiff spectrum tables given in Appendix I of the "photon difference" paper by Katz and Cameron,⁶ which has been multiplied by a varying conversion factor to change the basis of normalization from "roentgen" to the ion chamber integrated current which was used here. The effect of the changes in bremsstrahlung spectrum outlined above on the isochromats would be to make them more linear with energy near their lower ends.

Let us now consider the appearance of the activation curve which would result from a photonuclear cross section which consisted only of fairly widely spaced discrete levels. A set of such assumed levels is shown in Fig. 6(a). In Fig. 6(b) the isochromats of the bremsstrahlung spectrum corresponding to the energies of these levels are plotted, as well as the sum of these isochromats. This sum would constitute the activation curve observed in an experiment. The resulting shape of the activation curve consists of a number of segments, each concave towards the energy axis, separated by discontinuities of slope. This appearance is reminiscent

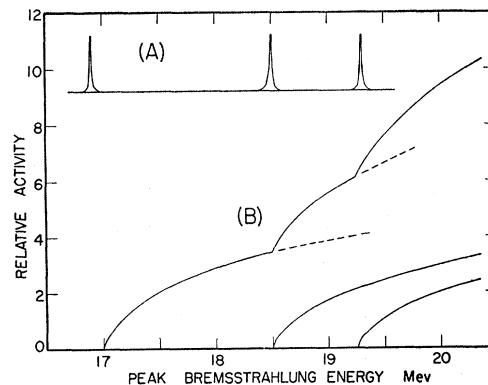


FIG. 6. Schematic representation to show how narrow levels and the isochromats can give rise to discontinuities in the activation curve.

⁷ L. I. Schiff, Phys. Rev. **83**, 252 (1951).

⁸ It is of interest to note that all the measurement of spectrum shape to date [H. W. Koch and R. E. Carter, Phys. Rev. **77**, 165 (1950); K. Phillips, Proc. Phys. Soc. (London) **A65**, 57 (1952); and Motz, Moller, and Wychoff, Phys. Rev. **89**, 968 (1953)] can be fitted with a straight line in the upper energy region to within experimental accuracy. This region extends over about the upper $\frac{1}{3}$ of the curve.

of the shape of the $O^{16}(\gamma,n)O^{15}$ activation curve at intermediate energies. A straightening of the isochromats in their initial portion for reasons outlined above, followed by a curved portion, may well give rise to the observed activation curves.

Equation (2) may be used to calculate the approximate value of $\int \sigma_i dE$ at each break. The first term on the right-hand side of this equation represents the activation curve without the contribution from the level at E_i and may be expected to lie at energies $E_0 > E_i$ along the extrapolation of the curve. The second term on the right-hand side thus represents the distance between the extrapolated and measured curves. Let this distance be $\Delta\alpha(E_0)$; then from (2) we find

$$G \int_0^{E_0} \sigma_i dE = \frac{\Delta\alpha(E_0)}{0.602P(E_i, E_0)}. \quad (4)$$

Values of this integral at the various breaks in the oxygen curve are given in Table I. For ease of com-

TABLE I. Integrated cross sections under the breaks.

E_i Mev	Carbon $G \int \sigma_i dE$ Mev-barn	E_i Mev	Oxygen $G \int \sigma_i dE$ Mev-barn
19.3	0.23×10^{-3}	15.9	0.06×10^{-3}
19.8	0.66	16.4	0.05
20.1	1.2	16.7	0.18
20.5	1.4	16.9	0.95
20.7	2.0	17.1	0.80
21.1	5.2	18.9	0.66
21.6	5.8	19.3	1.5
22.4	5.5	20.7	2.1
22.8	33.0	21.9	7.5
	0.055 Mev-barn		0.014 Mev-barn

putation we have taken E_0 in each case to be $E_i + \frac{1}{2}$ Mev. The values of $P(E_i, E_0)$ were obtained from an accurate set of graphs similar to those published by Johns *et al.*⁹ These values of $P(E_i, E_0)$ are given as a function of E_i in Fig. 7. Similar computations for the carbon breaks are also listed in Table I. The values listed are probably accurate to within a factor of 2. Two facts are immediately evident from this table: (a) the strength of the levels measured increases with increasing energy, with the last level given being by far the largest; and (b) the sum of these strengths is comparable to the integrated cross section when the activation curve is solved by the photon difference method⁶ as if it had no fine structure. Thus, the most recent value of $\int_0^{24} \sigma_{\gamma n} dE$ for carbon given by Montalbetti *et al.*¹⁰ is 0.029 Mev-barn and $\int_0^{22} \sigma_{\gamma n} dE$ for oxygen is 0.015 Mev-barn. These values are to be compared to 0.055 and 0.014 Mev-barn, respectively, from Table I. These results would imply that a substantial fraction of the $O^{16}(\gamma,n)O^{15}$ and $C^{12}(\gamma,n)C^{11}$

⁹ Johns, Katz, Douglas, and Haslem, Phys. Rev. **86**, 1062 (1950).

¹⁰ Montalbetti, Katz, and Goldemberg, Phys. Rev. **91**, 659 (1953).

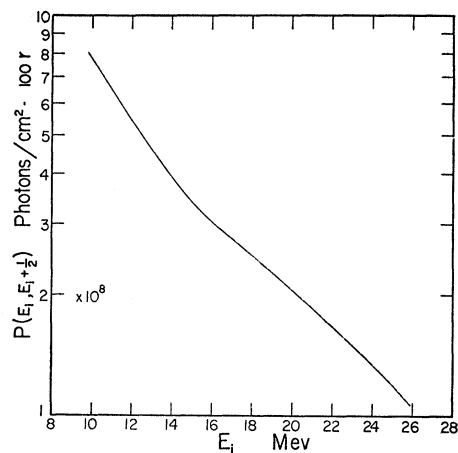


FIG. 7. Number of photons at the indicated energy per cm^2 per 100 r of irradiation, if the peak bremsstrahlung energy is $\frac{1}{2}$ Mev higher than the indicated energy.

reaction cross section takes place by photon absorption into nuclear levels which are located at the energies of the breaks in the activation curves.

In Fig. 8 we have plotted the cross-section curve for the $O^{16}(\gamma,n)O^{15}$ reaction previously published¹⁰ and have superposed on it our activation curve showing the positions of the levels and their relative strengths for comparison.

It would be desirable to check the existence of the resonances found here by some independent method. Unfortunately the excitation energies involved are so high that very little work has been done in this energy region with other kinds of bombarding particles. In a study of the reaction $B^{11}(p,n)C^{11}$, Blaser *et al.*¹¹ have found excitation energies of 19.4, 20.7, 21.4, and 21.8 Mev in the compound nucleus C^{12} . The first two of these agree well with the break positions found for

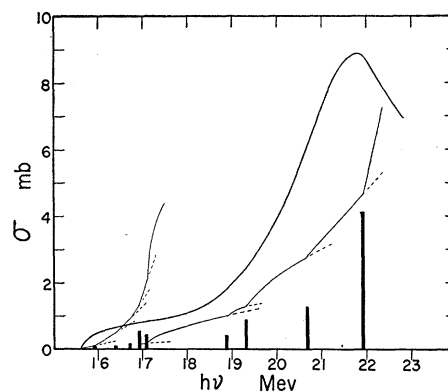


FIG. 8. $O^{16}(\gamma,n)$. Gamma-neutron cross section in O^{16} obtained from the activation curve using the photon difference method of analysis. Superposed on this cross section is the activation curve showing the positions of the breaks and a series of lines representing the relative integrated area under the corresponding breaks as listed in Table I.

¹¹ Blaser, Boehm, Marimier, and Scherrer, Helv. Phys. Acta **24**, 30 (1951).

C¹²(γ, n)C¹¹ reaction but a break at 21.6 Mev in our curve might be a combination of the last two resonances. On the basis that only "strong" breaks are likely to be resolved (except possibly near threshold), it is reasonable to suppose that most of the corresponding resonances involve electric dipole absorption. Thus the strong resonances in C¹² would have one unit of angular momentum and odd parity. It is believed that the ground state of B¹¹ is $\frac{3}{2}^-$. Thus the capture of S-wave protons should lead to 1⁻ and 2⁻ levels in C¹², and the capture of protons with higher orbital angular momentum would lead to additional kinds of states. For this reason one would expect many more resonances to be found in the B¹¹(p, n)C¹¹ reaction than in the C¹²(γ, n)C¹¹ reaction. The fact that the opposite is true is somewhat disturbing, but Blaser *et al.* did not have high-energy resolution for their protons, and it is possible that they missed many resonances.

Goward and Wilkins¹² have examined the C¹²($\gamma, 3\alpha$) and O¹⁶($\gamma, 4\alpha$) reactions using nuclear plates and have found fine structure in the cross sections for these reactions. In the C¹²($\gamma, 3\alpha$) reaction they found cross section peaks at 19.6, 20.7, 21.9, 23.1, and 24.3 Mev [as well as some below our (γ, n) threshold]. They were not able to resolve any levels in the oxygen reaction over the energy region covered by our experiments. It is difficult to estimate the accuracy to which the positions of these C¹² levels have been determined. The authors state that their resolution was probably of the order of 1 Mev, and possibly for this reason our results indicate about twice as many levels in the same energy range.

¹² F. K. Goward and J. J. Wilkins, Atomic Energy Research Establishment Report A.E.R.E. G/M 127 Harwell, Berks, England, March 24, 1952 (unpublished).

Fine Structure in the Neutron Yield Curves from (γ, n) Reactions in Li⁷, C¹², O¹⁶, and F¹⁹

J. GOLDEMBERG* AND L. KATZ

Department of Physics, University of Saskatchewan, Saskatoon, Canada

(Received April 7, 1954)

Fine structure previously observed in the β^+ activation curves of C¹¹ and O¹⁵ resulting from the betatron induced reactions C¹²(γ, n)C¹¹ and O¹⁶(γ, n)O¹⁵ is shown to be present in the neutron yield curves from these reactions by detecting the emitted neutrons. The position of this fine structure as a function of betatron operating energy is the same in both cases to within experimental accuracy. The Li⁷(γ, n)Li⁶ and F¹⁹(γ, n)F¹⁸ were examined and discontinuities in the neutron yield curves were found at 9.6, 10.8, 12.4, 14.0, and 17.5 Mev for the first reaction and 11.0, 11.5, 11.9, and 15.3 for the second.

INTRODUCTION

IN the accompanying paper we report on the fine structure observed in the *activity* curves resulting from the C¹²(γ, n)C¹¹ and O¹⁶(γ, n)O¹⁵ reactions induced by betatron irradiation. In those experiments the activity of the residual nuclei C¹¹(20.5 min) and O¹⁵(2.0 min) are plotted as a function of maximum bremsstrahlung energy. Since the presence of fine structure in the curves was indicated by changes in slope, their real existence and precise location requires that they be reproduced under varying experimental conditions and with different measuring techniques. For this reason and because many of the light nuclei do not have convenient half-lives for measuring their residual activity an apparatus previously built for detecting neutrons emitted in (γ, n) reactions¹ was slightly modified to give a high counting rate for improved accuracy and neutron yields for a number of elements were examined

for fine structure. The results of these measurements are reported in this paper.

EXPERIMENTAL TECHNIQUES

To measure the fine structure reported in this paper an energy stability of ± 5 kev in the control of the maximum bremsstrahlung energy is imperative during any one irradiation. A dispersion of over ± 30 kev, though not wiping out this fine structure, certainly makes it very difficult to detect. Recent experiments have indicated that a change of 1°C in the operating temperature of the betatron core, or a change in frequency of 0.15 cps in our 180-cps supply corresponds to an energy change of about 5 kev. All measurements reported were taken under conditions where we believe a stability of ± 5 kev was achieved.

A sketch of the experimental setup with all pertinent dimensions is shown in Fig. 1. The operation of this system has been previously described.¹ To obtain high counting rates two BF₃ counters were connected in parallel and large samples were used. Photon absorption in the samples does not alter the neutron yield curve

* Now at Departamento de Fisica, Faculdade de Filosofia, Ciencias e Letras, Universidade de Sao Paulo, Sao Paulo, Brazil, South America.

¹ Montalbetti, Katz, and Goldemberg, Phys. Rev. **91**, 659 (1953).